Biomedicine & Pharmacotherapy 167 (2023) 115503

Contents lists available at ScienceDirect

Biomedicine & Pharmacotherapy

journal homepage: www.elsevier.com/locate/biopha

Chronic exposure to L-BMAA cyanotoxin induces cytoplasmic TDP-43 accumulation and glial activation, reproducing an amyotrophic lateral sclerosis-like phenotype in mice

Serenella Anzilotti [a,1], Valeria Valente [b,1], Paola Brancaccio [c], Cristina Franco [a], Antonella Casamassa [d], Giovanna Lombardi [a], Alessandra Palazzi [b], Andrea Conte [b], Simona Paladino [b], Lorella Maria Teresa Canzoniero [a], Lucio Annunziato [d], Giovanna Maria Pierantoni [b,*,2], Giuseppe Pignataro [c,**,2]

[a] Department of Science and Technology, University of Sannio, 82100 Benevento, Italy
[b] Department of Molecular Medicine and Medical Biotechnology, School of Medicine, "Federico II" University of Naples, Italy
[c] Division of Pharmacology, Department of Neuroscience, Reproductive and Odontostomatological Sciences, School of Medicine, "Federico II" University of Naples, Italy
[d] IRCCS SYNLAB SDN S.p.A., 80143 Naples, Italy

ARTICLE INFO

Keywords:
l-BMAA
Mice
Amyotrophic Lateral Sclerosis
Neurodegeneration
Behavioral tests
Cyanotoxin

ABSTRACT

Background: Amyotrophic lateral sclerosis (ALS) is a progressive and often fatal neurodegenerative disease characterized by the loss of Motor Neurons (MNs) in spinal cord, motor cortex and brainstem. Despite significant efforts in the field, the exact pathogenetic mechanisms underlying both familial and sporadic forms of ALS have not been fully elucidated, and the therapeutic possibilities are still very limited. Here we investigate the molecular mechanisms of neurodegeneration induced by chronic exposure to the environmental cyanotoxin L-BMAA, which causes a form of ALS/Parkinson's disease (PD) in several populations consuming food and/or water containing high amounts of this compound.

Methods: In this effort, mice were chronically exposed to L-BMAA and analyzed at different time points to evaluate cellular and molecular alterations and behavioral deficits, performing MTT assay, immunoblot, immunofluorescence and immunohistochemistry analysis, and behavioral tests.

Results: We found that cyanotoxin L-BMAA determines apoptotic cell death and a marked astrogliosis in spinal cord and motor cortex, and induces neurotoxicity by favoring TDP-43 cytoplasmic accumulation.

Conclusions: Overall, our results characterize a new versatile neurotoxic animal model of ALS that may be useful for the identification of new druggable targets to develop innovative therapeutic strategies for this disease.

1. Introduction

Amyotrophic lateral sclerosis (ALS) is a progressive and devastating neurodegenerative disease characterized by the loss of Motor Neurons (MNs) in spinal cord, motor cortex and brainstem [1–3]. Usually, the disease shows an onset peak around 45–60 years and has a post-diagnosis survival time of approximately 3–5 years [2]. Nonetheless, ALS is a clinically heterogeneous pathology, and some patients present a less aggressive disease and survive longer. Clinically, the loss of motor neurons is associated to progressive muscle weakening and

Abbreviations: ALS, Amyotrophic lateral sclerosis; L-BMAA, β-N-methylamino-L-alanine; Wt, Wild type; TDP-43, TAR DNA-binding protein 43; MNs, Motor Neurons; PB, phosphate buffer; Bcl2, B-cell lymphoma 2; FTD, Frontotemporal Dementia; C9ORF72, chromosome 9 open reading frame 72; SOD1, Cu/Zn superoxide dismutase; FUS/TLS, Fused in sarcoma/translocated in liposarcoma; GFAP, Glial fibrillary acidic protein; Iba1, Ionized calcium-binding adapter molecule 1; DAB, Standard 3,3′-diaminobenzidine; AU, Arbitrary units; NeuN, Neuronal nuclei.

* Correspondence to: Department of Molecular Medicine and Medical Biotechnology, University of Naples "Federico II", Via Pansini 5, 80131 Naples, Italy.
** Correspondence to: Division of Pharmacology, Department of Neuroscience, School of Medicine, "Federico II", Via Pansini 5, 80131 Naples, Italy.
E-mail addresses: gmpieran@unina.it (G.M. Pierantoni), giuseppe.pignataro@unina.it (G. Pignataro).
[1] Co-first authors.
[2] Co-last and co-corresponding authors.

https://doi.org/10.1016/j.biopha.2023.115503
Received 29 May 2023; Received in revised form 24 July 2023; Accepted 12 September 2023
Available online 18 September 2023

fasciculation. In the later disease stages, the patients become paralyzed. Furthermore, up to 50 % of ALS patients show cognitive impairment and mild memory decline [3]. Ultimately, ALS induces paralysis and premature death which is generally caused by respiratory failure [3–5]. The neuropathological hallmarks of this neuromuscular disorder are degeneration of motor neurons in the spinal anterior horn and motor cortex and loss of axons in the lateral columns of the spinal cord [6]. Based on the inheritance of the disease, ALS is classified in two forms: the sporadic form (sALS), which includes the majority of ALS cases, and the familiar form (fALS), which represents about 5–10 % of the cases [7,8].

A specific form of ALS associated to dementia and Parkinson's features has been observed with high frequency in restricted groups of people such as the Chamorro of Guam and surrounding Mariana Island [9]. Attempts to determine the etiology of the disease included investigations of common dietary elements for potential neurotoxins, which led to Vega and Bell's (1967) isolation of 2-amino-3-(methylamino)propanoic acid, also called β-N-methylamino-L-alanine (BMAA). Acute neurotoxicity was subsequently demonstrated in chicks and rats [10], making BMAA a candidate for the causative agent of what had come to be known as amyotrophic lateral sclerosis/parkinsonian dementia complex (ALS/PDC). In fact, these populations consume food containing high amount of L-BMAA and drinking water primarily deriving from eutrophic reservoirs with phytoplankton dominated by potentially toxic *Cyanobacteria* [11] and L-BMAA has been detected in natural water samples and in cyanobacterial cell cultures derived from cell isolated from these reservoirs [12]. Although the causal role of L-BMAA in triggering ALS/PDC features is debated [13–19], we and others previously demonstrated that L-BMAA exposure may induce a typical picture of ALS *in vitro* [20–22]. Nonetheless, the molecular mechanisms of neurodegeneration associated to L-BMAA exposure are not fully described and L-BMAA-based neurotoxic *in vivo* models of ALS have not been characterized yet. Even though the molecular mechanisms underlying the pathogenesis of both sALS and fALS have not been fully elucidated, and they can be diverse for different forms of ALS, it is known that almost all ALS cases are characterized by specific molecular alterations. In particular, the dysregulation of the transactive response DNA-binding protein −43 (TDP-43), a ubiquitously expressed DNA/RNA-binding nuclear protein involved in RNA metabolism, transport, and stability, is found in almost all ALS patients. In fact, regardless of the sporadic or familiar nature of the disease, increased levels of TDP-43 expression and its cytoplasmic delocalization and accumulation are molecular hallmarks of ALS. The dysregulation of TDP-43 dynamics is a key pathogenetic feature not only of ALS but also of other neurodegenerative diseases, such as Frontotemporal Dementia (FTD) [23]. Differently from ALS, FTD is characterized by progressive neuronal loss in the frontal and temporal cortices associated to personality and behavioral changes. However, ALS and FTD share similar molecular signatures. In particular, TDP-43 is recognized as a major component of cytoplasmic inclusions for ~98 % of ALS and ~50 % of FTD patients [24]. Since the biogenesis of these inclusions remains unknown, it should be considered that environmental risk factors may play a causal role in this process. Several *in vitro* and *in vivo* studies suggest that exposure to the environmental cyanotoxin β-Methylamino-L-alanine (L-BMAA) results in TDP-43 increased expression and cytoplasmic accumulation [25]. Overall, understanding the mechanisms of L-BMAA toxicity may be of relevance also for the identification of innovative therapeutic strategies for ALS. Currently, there are no fully satisfactory treatments for ALS. In fact, the only two drugs approved for ALS, namely the NMDA blocker riluzole and the ROS scavenger edaravone, only prolong life expectancy for less than 3 months [26,27]. Based on this evidence, in this paper we investigated the effects of chronic administration of L-BMAA in human SH-SY5Y neuroblastoma cells and in mice, finding that the treatment with this cyanotoxin recapitulates many ALS characteristics in both systems. In fact, L-BMAA has a cytotoxic effect on SH-SY5Y cells, which is associated to TDP-43 expression increase and cytoplasmic accumulation. Consistently, L-BMAA-treated mice present an ALS-like phenotype characterized by an increase in TDP-43 total and cytoplasmic expression, apoptotic cell death and astrogliosis in spinal cord and motor cortex, and behavioral abnormalities, such as poor motor coordination and balance and altered spatial and recognition memory.

2. Methods

2.1. L-BMAA treatment in mice

C57BL/6 mice were chronically treated with different doses of L-BMAA. Experimental groups of 10 mice (at 10 weeks of age) were administered with intraperitoneal injections of 1 and 30 mg/Kg of L-BMAA or vehicle each day for 30 days. General health status and motor capability/neurological assessment was carried out at the end of each week by performing specific behavioral tests.

Additional experimental groups were administered with 30 mg/Kg of L-BMAA or vehicle each day for 30 days and were sacrificed at the end of treatment for immunohistochemical and biochemical investigations.

Overall, 60 male mice were housed in microisolator caging under standard 12 h light–dark conditions with access to food and water. 6 mice out of 60 animals were not included in the experimental groups as they died for unknown reasons. Dead animals were equally distributed among the experimental groups. Experiments were performed according to the international guidelines for animal research and approved by the Animal Care Committee of "Federico II" University of Naples, Italy and Ministry of Health, Italy. All efforts were made to minimize animal suffering and to reduce the number of animals used.

2.2. Cell cultures

Human neuroblastoma SH-SY5Y cells were grown in RPMI medium (Euroclone, Cat. #ECB2000) supplemented with 10 % Fetal Bovine Serum (CytivaHyClone™, Cat. #SH30070.03IH25-40) and L-glutamine (Euroclone, Cat. #ECB3000). Cells were maintained at 37 °C in a saturated humidity atmosphere containing 95 % air and 5 % CO_2.

2.3. L-BMAA exposure and cell viability measurement

Chronic exposure to L-BMAA in SH-SY5Y cells was simulated performing subsequential toxin stimulations as follows: cells were starved for 6 h in a serum-free medium followed by stimulation with 2 mML-BMAA complete medium after 24 h and 48 h from seeding. After 72 h or 96 h of L-BMAA exposure cells were harvest and analyzed. Cell viability was evaluated by MTT (3[4,5-dimethylthiazol-2-yl]−2,5-diphenyltetrazolium bromide) assay.

2.4. Nuclear/cytoplasmic fractionation

SH-SY5Y cells nuclear/cytoplasmic fractionation was obtained using ReadyPrep™ Protein Extraction Kit (Bio-Rad, Cat. #1632089) according to manufacturer instructions. Briefly, SH-SY5Y cells grown on petri dishes were scraped with CPEB buffer, leaved on ice for 30 min and centrifuged at 1000 *g* for 30 min. The supernatant containing the cytoplasmic fraction was collected. The pellet was solved in PSB buffer, vortexed and centrifuged at 12,000*g* for 20 min and the supernatant containing the nuclear fraction collected.

2.5. Western blotting and antibodies

SH-SY5Y cells and tissues were lysed with lysis buffer RIPA as previously described [28]. Total protein extracts were separated by SDS-PAGE and transferred onto nitrocellulose transfer membranes (Perkin Elmer, Cat. #NBA085C001EA). Membranes were blocked with 5 % BSA (bovine serum albumin protein in TBS 1 % buffer, 0.02 % sodium

azide) and incubated with antibodies at the appropriate dilutions. The filters were incubated with horseradish peroxidase-conjugated secondary Antibodies, and the signals were detected with ECL (Thermo Fisher Scientific, Cat. #32106). The antibodies used for western blotting were as follows: polyclonal anti-TDP-43 (Proteintech, Cat. #10782–2-AP), polyclonal anti-calnexin (Enzo Lifescience, Cat. #ADI-SPA-860-F), monoclonal anti-Sp3 (Santa Cruz, Cat. #365038), monoclonal anti-GAPDH (Santa Cruz, Cat. #32233). Anti β-Tubulin (Sigma-Aldrich, Cat. #T8328.

2.6. RNA extraction and quantitative RT-PCR

Total RNA isolation was performed using the TRI-reagent solution (Merck Life Science). cDNA was synthesized from 1 μg of total RNA using the QuantiTect Rev. Transcription Kit.

(Qiagen). qRT-PCR was performed using the FluoCycle Master Mix (Euroclone). All these procedures were conducted according to manufacturer's instructions. Gene-specific primers used for amplification were as follows:

TDP-43-Fw: 5′- AATTCTGCATGCCCCAGAT −3′;.

TDP-43-Re: 5′- CGGATGTTTTCTGGACTGCT −3′;.

GAPDH -Fw: 5′- TGCACCACCAACTGCTTAGC −3′;.

GAPDH-Re: 5′- GGCATGGACTGTGGTCATGAG −3′.

The relative expression levels were calculated by using the 2–ΔΔCT formula.

2.7. Tissue processing, immunostaining, and confocal immunofluorescence

Animals were anesthetized and transcardially perfused with saline solution containing 0.01 ml heparin, followed by 4 % paraformaldehyde in 0.1 mol/l PBS saline solution. Brains and spinal cord were processed as previously described [20]. Spinal cords and brains were rapidly removed on ice and postfixed overnight at + 4 °C and cryoprotected in 30 % sucrose in 0.1 M phosphate buffer (PB) with sodium azide 0.02 % for 24 h at 4 °C. Next, spinal cords and brains were sectioned frozen on a sliding cryostat at 40 μm thickness, in rostrum-caudal direction. Afterwards, free floating serial sections were incubated with PB Triton X 0.3 % and blocking solution (0.5 % milk, 10 % FBS, 1 % BSA) for 1 h and 30 min. The sections were incubated overnight at + 4 °C with the following primary antibodies: anti-SMI32 (Biolegend cat #SMI-32P), anti-TDP-43 (Proteintech, Cat. #10782–2-AP), anti-GFAP (Abcam, cat #AB7260), anti-IBA1 (Wako, cat #019–19,741). The sections were then incubated with the corresponding florescent-labeled secondary antibodies, Alexa 488/Alexa 594 conjugated antimouse/antirabbit IgG. Nuclei were counterstained with Hoechst. Images were observed using a Zeiss LSM700 META/laser scanning confocal microscope (Zeiss, Oberkochen, Germany). Single images were taken with a resolution of 1024 × 1024. Nissl staining was performed as previously described [20]. Briefly, slide-mounted sections were dipped 7 min in 0.5 % solution of Cresyl Violet in distilled water supplemented with acetic acid (16 N solution, 60 drops/l). Slides were then rinsed in distilled water, dehydrated through graded ethanol baths (95 %, 100 %; 5 min each), dilapidated 8 min in xylene, and coverslipped with Eukitt Mounting Medium. Standard 3,3′-diaminobenzidine (DAB) staining was employed on coronal step serial sections using antibody directed against TDP-43.

2.8. GFAP analysis

Frozen spinal cord was sectioned on a sliding cryostat at 20 μm, in lumbar spinal cord Images from the same areas of each spinal cord region were compared. Analyses were performed using image J software in the total number of positive signals of GFAP antibody for photographic field (mm2) in lumbar spinal cord (L1-L6) of vehicle and L-BMAA exposed mice. n = 3 mice per treatment group and three sections.

Quantification of TDP-43 fluorescence intensity on tissue sections at the level of the lumbar spinal cord (L1-L6), was quantified in terms of pixel intensity value by using the NIH image software, as previously described [29] Briefly, digital images were taken with × 40 or × 20 objective and identical laser power settings and exposure times were applied to all the photographs from each experimental set. Images were first thresholded to identify the positive signal; subsequently, the pixels expressing TDP-43 in cytoplasm and nucleus were identified. Finally, the number of pixels positive for TDP-43 in nucleus and cytosol was measured per microscope field. Images from the same areas of each spinal cord region were compared. Results were expressed in arbitrary units. n = 3 mice per treatment group and six sections.

2.9. Motor neurons counting analysis

MNs were counted in the spinal cord. Sections of each area were analyzed as previously described [30]. Frozen brain tissue and spinal cord were sectioned on a sliding cryostat at 20 μm, in rostrum-caudal direction. Analyses were performed using image J software in Polygonal-shaped neurons larger than 150–200 μm^2 with a well-defined cytoplasm, nucleus, and nucleolus for MNs counting. Quantification of MNs was determined by counting and averaging 4 sections selected at equally spaced intervals spanning L1–6 under 20× magnification, n = 6 mice for each experimental group were analyzed. Cell counting analysis was determined as total MNs per field (mm2) of vehicle and L-BMAA exposed mice.

2.10. T-maze spontaneous alternation

This procedure was carried out in an enclosed "T" shaped maze (Med Associated, St. Albans, VT) in which long arm of the T (47 cm × 10 cm) serves as a start arm and the short arms of the T (35 cm × 10 cm) serve as the goal arms. In this task the mouse was placed in the start arm and after 5 s the door was opened, and the mouse was allowed to choose and explore one of the goal arms. When the mouse had fully entered the choice arm (tail tip all the way in) a guillotine door was closed, and the mouse was confined to the choice arm for 30 s. The mouse was then removed, the guillotine door lifted, and the next trial initiated. This was repeated for a total of 10 trials. If the mouse did not make a choice within 2 min the trial was ended and advanced to the next. At the conclusion of each trial the maze was cleaned of urine and faeces [31].

2.11. Delay-dependent one-trial object recognition task and Open field test

The behavioral tests used in this study for assessing cognitive function were carried out in arenas (50 × 50 × 40 cm) resting on an infra-red emitting base. Mice behavior was recorded by an infrared-sensitive camera placed 2.5 m above the arenas and the data were analyzed using the tracking program Noldus. The object recognition task is based on propensity of mice to explore a novel object *versus* a previously experienced object (familiar) when allowed to explore freely. Briefly, two identical objects were placed in the arena and animals were allowed to explore them for 10 min. Testing occurred 24 h later in the same arena in which one of the original objects was replaced by a novel object. Object exploration was assumed as time spent in approaching an object (touching it with either mouse vibrissae, snout, or forepaws). The percentage of time spent exploring the novel object, compared with the total time spent exploring both objects, was considered as a measure of object recognition: discrimination index = t novel/(t novel + t familiar) X100 [32]. The open field test for the evaluation of locomotion, anxiety and stereotypical behaviors was performed as previously described [33].

2.12. Statistical analysis

Data were evaluated as means ± SEM. Student's t-test was used for two groups comparison. One Way Anova was used for motor behavioral

test. Statistical significance was accepted at the 95 % confidence level ($p < 0.05$). Statistical analyses were performed by using GraphPad Prism 5.0.

3. Results

3.1. L-BMAA exposure affects TDP-43 expression and subcellular localization in neuroblastoma SH-SY5Y cell line

To evaluate the toxic effects of L-BMAA exposure on human neuronal cells, we treated the neuroblastoma-derived SH-SY5Y cell line with 2 mM L-BMAA for 96 h (as described in the Methods section), and then we evaluated the treatment cytotoxicity performing a MTT assay. As shown in Fig. 1A, L-BMAA-treated cells showed a 50 % reduction of MTT-signal compared to control cells, indicating that L-BMAA exposure affected the survival of SH-SY5Y cells. Then, TDP-43 protein expression and sub-cellular distribution were evaluated performing immunoblot and immunofluorescence analysis (Fig. 1 B-C-D). As shown in Fig. 1B–D, upon L-BMAA exposure, both the total and the cytoplasmic amounts of TDP-43 protein increased, whereas the nuclear amount was not significantly affected (Fig. 1D).

Moreover, the immunofluorescence analysis showed a strong dotted cytoplasmic TDP-43 fluorescent signal in cells exposed to L-BMAA for 96 h (Fig. 1B). The same effect was observed also after 72 h of exposure to L-BMAA (Fig.S1).

In order to evaluate whether L-BMAA affects TDP-43 expression at transcriptional level, we analyzed its mRNA levels by qPCR. As shown in Fig. 1E, TDP-43 mRNA abundance is not significantly different between vehicle- and L-BMAA-treated cells. Taken together these results show that L-BMAA has a cytotoxic effect in SH-SY5Y cells which is associated to a post-transcriptional increase in total and cytoplasmic expression of TDP-43 protein.

3.2. L-BMAA treatment leads to TDP-43 cytoplasmic accumulation in mouse spinal cord motor neurons

To evaluate the neurotoxic consequences of the cyanotoxin L-BMAA exposure *in vivo*, C57BL/6 mice were chronically treated with increasing doses of L-BMAA. Experimental groups of 10 mice (at 10 weeks of age) were administered with intraperitoneal injections of 1 and 30 mg/Kg of

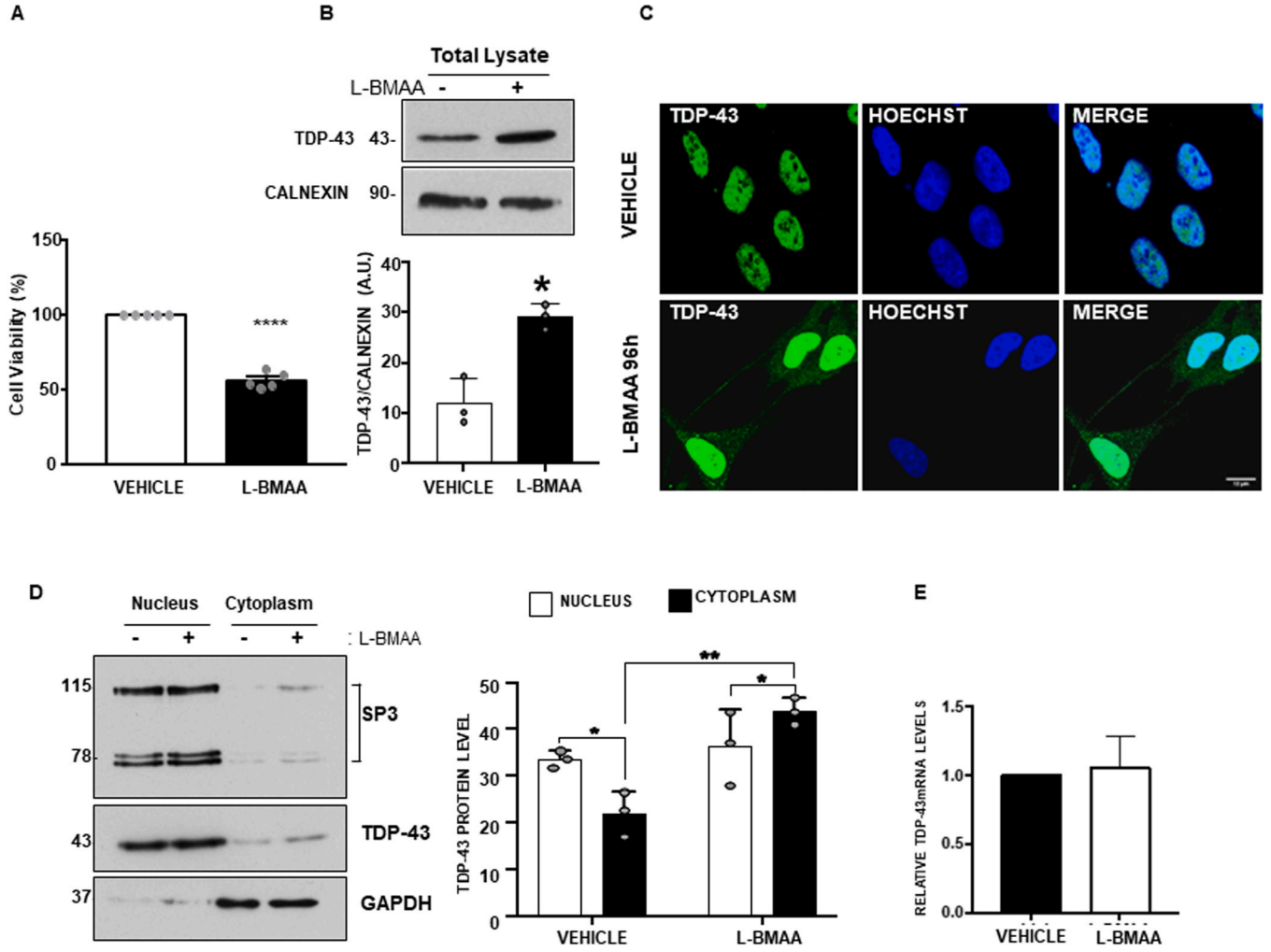

Fig. 1. Cell viability and TDP-43 sub-cellular localization in SH-SY5Y cells upon L-BMAA exposure. A) Cell viability of SH-SY5Y cells was assessed by MTT assay. B) Representative image of western blot analysis (top panel) and quantification of TDP-43 protein expression, arbitrary units (AU), (bottom panel) on total protein extracts from SH-SY5Y cells exposed to vehicle or L-BMAA (2 mM). The calnexin expression level was used for normalization. C) Immunofluorescence analysis of TDP-43 in SH-SY5Y cells exposed to vehicle or L-BMAA (2 mM). Nuclei were labeled with Hoechst dye. Original magnification 40X, scale bar = 12 μm D) Representative image of western blot analysis (left panel) and quantification of TDP-43 protein expression, arbitrary units (AU), (right panel) on nucleus/cytoplasm fractionation of SH-SY5Y cells exposed to vehicle or L-BMAA (2 mM). Sp3 protein was used as control for the nuclear fraction, GAPDH for the cytoplasm fraction. E) TDP-43 mRNA expression in SH-SY5Y cells exposed to vehicle or L-BMAA (2 mM) was analyzed by qRT-PCR. Data are expressed as mean ± SEM (n = 3 for each group). $*p < 0.05$ $**p < 0.01$ $***p < 0.001$.

L-BMAA or vehicle each day for 30 days, monitoring general health status and motor capabilities at the end of each of the four weeks. L-BMAA exposure did not affect mice body weight at any dosages, and no significant neurodegenerative features were observed for 1 mg/Kg of L-BMAA (Fig. S2). Therefore, all the following experiments were conducted using 30 mg/Kg of L-BMAA. Since exposure to L-BMAA is known to induce cytoplasmic delocalization of TDP-43 in rat models [25], we evaluated whether this compound could cause TDP-43 accumulation also in the soma of mouse MNs. To this aim, TDP-43 expression levels and subcellular distribution were evaluated by immunostaining and immunoblot analysis of spinal cord sections from L-BMAA- and vehicle-treated mice. As shown in Fig. 2 A-B, TDP-43 signal was much stronger in the spinal MNs of L-BMAA-treated mice than in those of control ones. Moreover, aggregates of cytoplasmic TDP-43 were clearly visible in the spinal cord of animals treated with 30 mg/Kg of LBMAA (Fig. 2A see arrows). In addition, to evaluate TDP-43 subcellular distribution in mouse MNs, a double immunofluorescence analysis was performed using anti-TDP-43 and anti-SMI32 (as MNs marker) antibodies on spinal cord sections from L-BMAA and vehicle-treated mice (Fig. 2 C–J). As expected, an increase in TDP-43 cytoplasmic signal was found in spinal SMI32-positive MNs from L-BMAA-treated mice with respect to their vehicle-treated counterpart (Fig. 2 D,H). Furthermore, confocal microscopy experiments were quantified, as seen in the graph (Fig. 2K) the intensity of TDP-43 fluorescence increased in the cytosol of L-BMAA treated mice compared to vehicles ones while in the nucleus there was a reduction of the TDP-43 signal in L-BMAA mice. In order to investigate whether the treatment with L-BMAA influenced TDP-43 expression and subcellular distribution also in cortical neurons, immunoblotting, and immunofluorescence analysis were performed on motor-cortex sections from vehicle and L-BMAA-treated mice. The TDP-43 immunoblot analysis (Fig. 3A) and the double immunofluorescence assay using anti-NeuN and anti-TDP-43 antibodies showed an increase in total TDP-43 levels and its cytoplasmic localization in treated NeuN-positive neurons compared to the untreated counterpart (Fig. 3 B–J). All together, these data indicate that L-BMAA chronic exposure causes TDP-43 over-expression and cytoplasmic accumulation in mouse

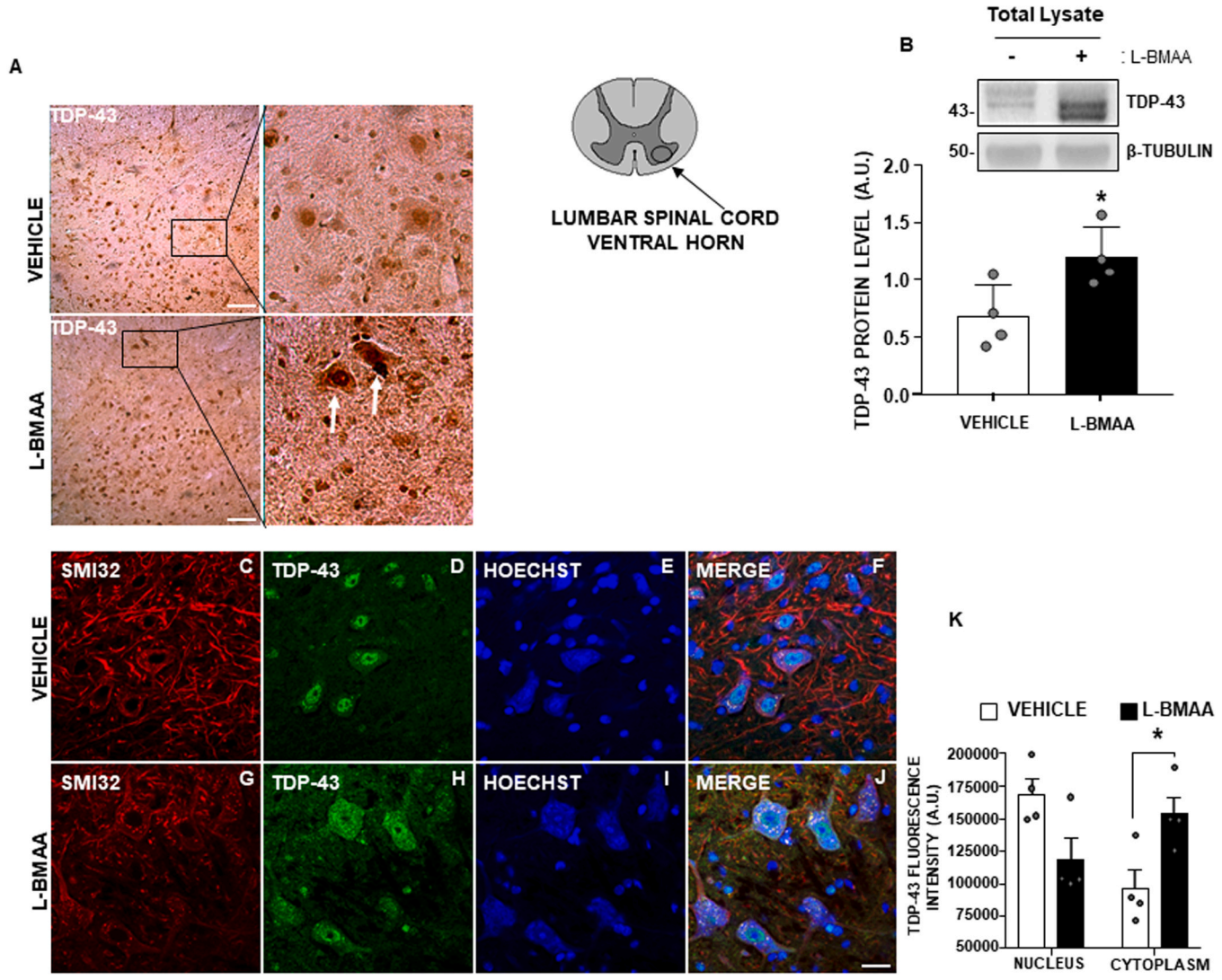

Fig. 2. TDP-43 expression pattern in mice spinal MNs upon L-BMAA exposure. Representative image of TDP-43 3,3′-diaminobenzidine (DAB) staining on spinal cord. Original magnification, 10X (Scale bar 100 μm). Magnified views of DAB staining are shown. TDP-43 cytoplasmic deposits are indicated by arrows. B) Representative image of western blot analysis (top panel) and quantification of TDP-43 protein expression, arbitrary units (AU), (bottom panel) on total protein extracts from spinal cord. The β-tubulin expression level was used for normalization. Data are expressed as mean ± SEM (n = 4/5 for each group). * $p < 0.05$. C,G) Immunofluorescence analysis of SMI32 from mice treated with vehicle or L-BMAA (30 mg/Kg). D,H) TDP-43 labeling in green, E,I) nuclei were labelled with Hoechst dye F,J) Merge images. K) Quantification of nuclear and cytoplasmic TDP-43 fluorescence intensity, arbitrary units (AU). Data are expressed as mean ± SEM (n = 4 for each group). *$p < 0.05$ Error bars ± SEM; for statistical analysis, Student's t test was used, *$p < 0.05$. Original magnification, 40X. Scale bar = 20 μm.

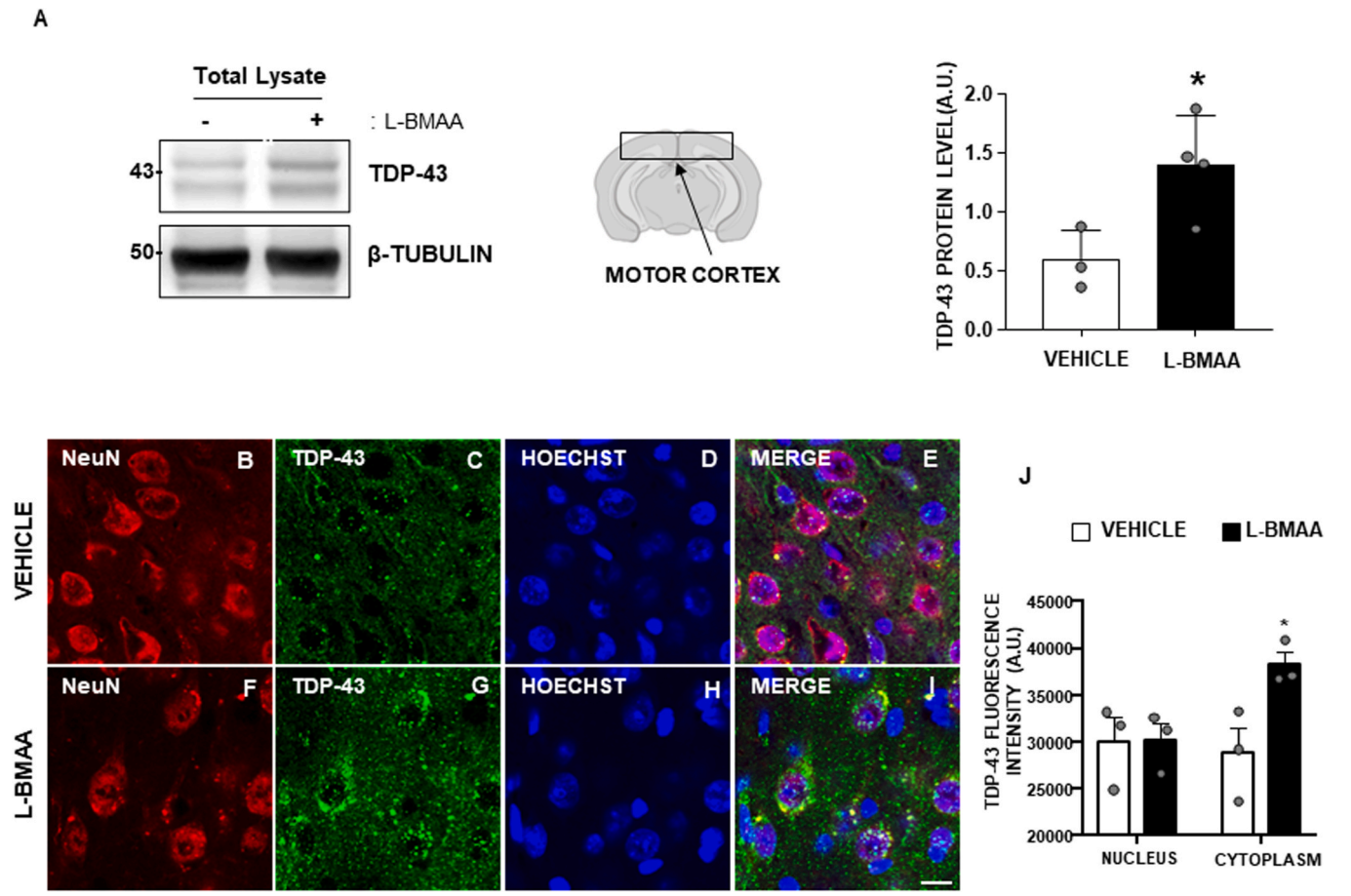

Fig. 3. TDP-43 expression pattern in mice motor cortex upon L-BMAA exposure . Representative image of western blot analysis (left panel) and quantification of TDP-43 protein expression, arbitrary units (AU), (right panel) on total protein extracts from motor cortex. The β-tubulin expression level was used for normalization. Data are expressed as mean ± SEM (n = ¾ for each group). *$p < 0.05$. B,F) Immunofluorescence analysis of NeuN in motor cortex from mice treated with vehicle or L-BMAA (30 mg/Kg). C,G) Immunofluorescence analysis of TDP-43. D,H) Nuclei were labeled with Hoechst dye. Merge images in E,I. J) Quantification of nuclear and cytoplasmic TDP-43 fluorescence intensity, arbitrary units (AU). Data are expressed as mean ± SEM (n = 3 for each group). *$p < 0.05$ Error bars ± SEM; for statistical analysis, Student's t test was used. Original magnification, 40X. Scale bar = 20 μm.

motor and cortical neurons.

3.3. L-BMAA treatment induces motor neuron death in mouse ventral spinal horn

In order to investigate whether the TDP-43 upregulation and cytoplasmic accumulation in L-BMAA-treated mouse spinal cord motor neurons are associated to MNs loss, mice spinal cord sections were stained with Nissl, and the number of MN was evaluated in the ventral spinal cord region. Since in ALS pathophysiology the degeneration occurs preferentially in large MNs, we specifically counted the number of cells with a perikaryal projection area bigger than 200 μm^2 (Fig. 4A). L-BMAA-treated mice showed lower number of spinal MNs (19 ± 1.5) with respect to the vehicle-treated counterpart (28.83 ± 1.4) (Fig. 4-B), suggesting that L-BMAA causes large MNs death in mice spinal cord.

Therefore, to evaluate whether the observed L-BMAA-induced decrease of spinal MN is associated to apoptosis activation, we evaluated the expression levels of caspase-3 proteins by immunoblotting analysis. As shown in Fig. 4C, the levels of caspase-3 active (cleaved) form were significantly higher in spinal cord from L-BMAA-treated compared to vehicle-treated mice. Collectively, these results revealed that L-BMAA chronic exposure leads to MNs loss associated to the activation of apoptotic cell death.

3.4. L-BMAA treatment induces astrogliosis in mouse spinal cord

Since neuronal death is typically associated to astrogliosis and microgliosis, to verify whether the L-BMAA-treatment causes an increase in astrocytes and/or microglia, GFAP immunostainings and immunoblot were performed on spinal cord sections from vehicle- and L-BMAA-treated mice. As shown in Fig. 5, the number of GFAP-positive cells was significantly higher in spinal cord from L-BMAA- than in vehicle-treated mice (Fig. 5 G). Consistently, the immunoblotting analysis revealed a strong increase in GFAP expression levels in spinal cord from L-BMAA-treated mice (Fig. 5 A,D). On the contrary, no difference in Iba1 expression levels was detected for L-BMAA-treated compared to vehicle-treated mice (Fig. S3). These results highlighted that severe astrogliosis but not microgliosis is observed upon L-BMAA chronic exposure in mice.

3.5. L-BMAA exposure induces ALS neurodegenerative symptoms in mice

To evaluate whether the above mentioned cellular and molecular alterations induced by L-BMAA exposure are associated to behavioral abnormalities typical of a ALS-like phenotype, we analyzed mouse motor coordination performing the Rotarod test. Interestingly, we found that L-BMAA treated mice showed poor motor coordination and balance (Fig. 6). In particular, L-BMAA-treated mice progressively showed an increased tendency to fall, starting from the first week, and reaching a

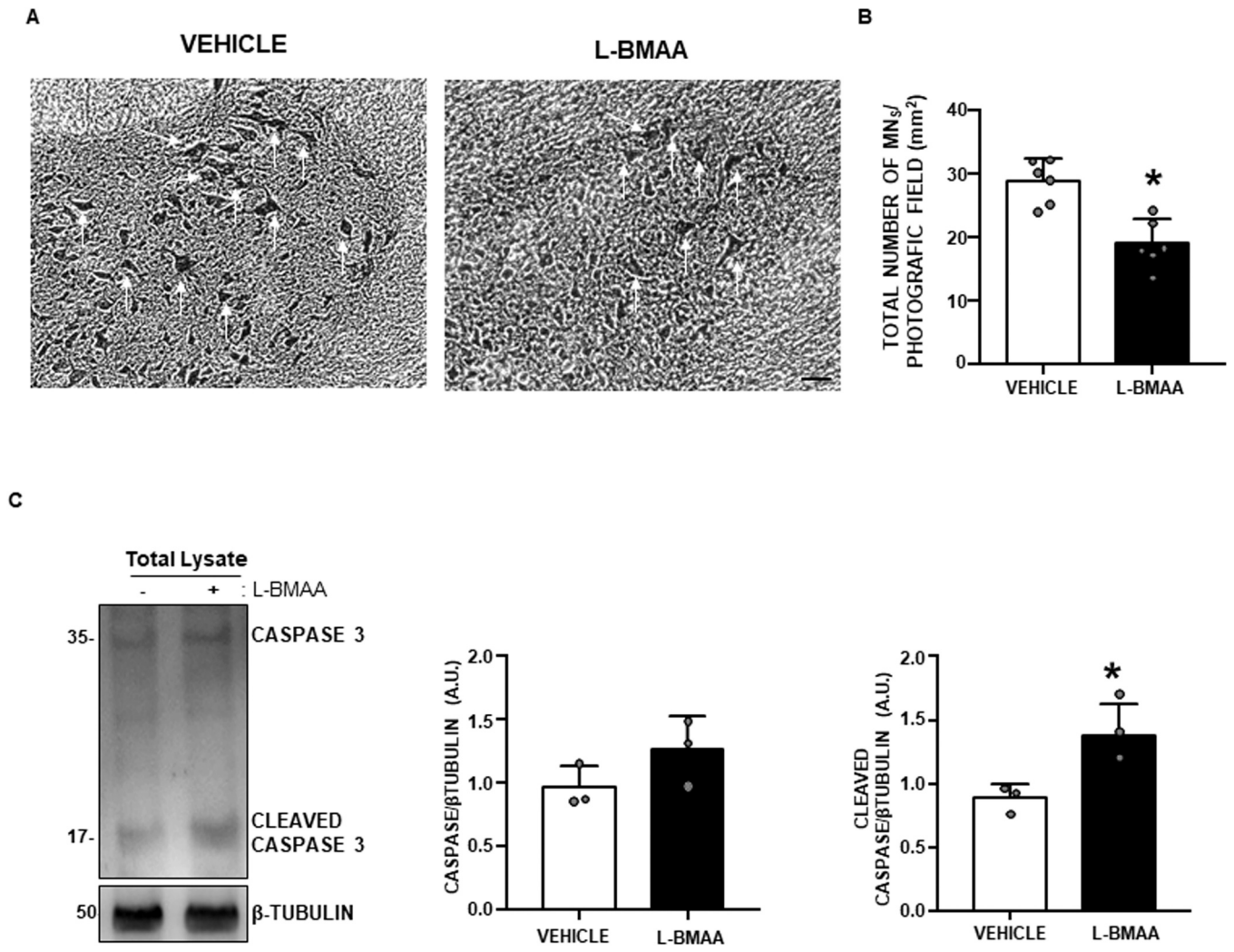

Fig. 4. L-BMAA impact on mice MNs survival. A) Representative image of Nissl staining of spinal cord sections from vehicle and L-BMAA exposed mice. B) Relative motor neurons counting analysis. Scale bar 100 μm 10x. (n = 6 for each group). C) Representative image of western blot analysis (left panel) and quantification of Caspase 3 full- length and cleaved protein expression, arbitrary units (AU), (right panel) on total protein extracts from spinal cord. The β-tubulin expression level was used for normalization. Data are expressed as mean ± SEM (n = 3 for each group). *p < 0.05

dramatic reduction (70 %) of the time spent on rod at the 4th week of treatment, whereas vehicle-mice showed a slightly improvement in the rotarod performance over time, as they learn how keep balance while on the rod (Fig. 6A). Furthermore, when tested for hindlimbs clasping, L-BMAA-treated mice displayed increasing duration of hindlimb retraction showing 1 min of clasping posture on a 3 min-test at the 4th week of treatment. Vehicle-treated mice did not show significant hindlimb retraction (Fig. 6B).

Hindlimb grip test was evaluated by placing the mouse on a grid upside-down and the latency to fall off the grid was measured up to a maximum of 60 s. For the L-BMAA-treated mice the loss of limb strength started to be evident after 2 weeks of treatment (40,1 ± 1 s) compared to vehicle mice (58,2 ± 1 s) (Fig. 6C). Furthermore, after 4 weeks of treatment, L-BMAA-treated mice failed the test after 20 s whereas vehicle mice completed the test (59,3 ± 0,5 s).

Altogether, these data indicate that 30-day long chronic treatment with 30 mg/Kg of L-BMAA leads to the progressive manifestation of motor behavior symptoms similar to those observed in mice with intermediate stage ALS.

3.6. Chronic exposure to L-BMAA leads to cognitive decline in mice

Since TDP-43 cytoplasmic accumulation is found also in FTD, we assessed whether L-BMAA exposure could impair mouse spatial and recognition memory, performing a set of cognitive tests, including open field test, object recognition test, and T-maze spontaneous alternation test.

In particular, to assess mice motor activity, we performed an open field test, placing each mouse in an experimental cage (50x50cm, 40 cm high), and allowing it to explore the cage for 10 min, while a video tracking system recorded the activity. The distance traveled and the time spent in the center of the cage were measured. L-BMAA-exposed mice showed a decreased motor activity, as the total distance traveled was reduced (Fig. 7A,B), compared to control group animals (Fig. 7A,C).

To evaluate also the recognition memory and the response to a novel environment, mice were assayed in an open field cage with two objects to explore while a video tracking system recorded the activity (object recognition test). During an initial training session, two identical objects were given to the mice, and the time spent exploring them was measured. 24 h after the removal of the objects, the mice were tested again providing them one of the objects with which they had interacted during the training session (familiar), and a new one (novel). The difference in the amount of time spent exploring the novel object rather than the familiar one (discrimination index) is indicative of short-term working memory. The discrimination index dramatically decreased for mice treated with L-BMAA, which spent much less time exploring the

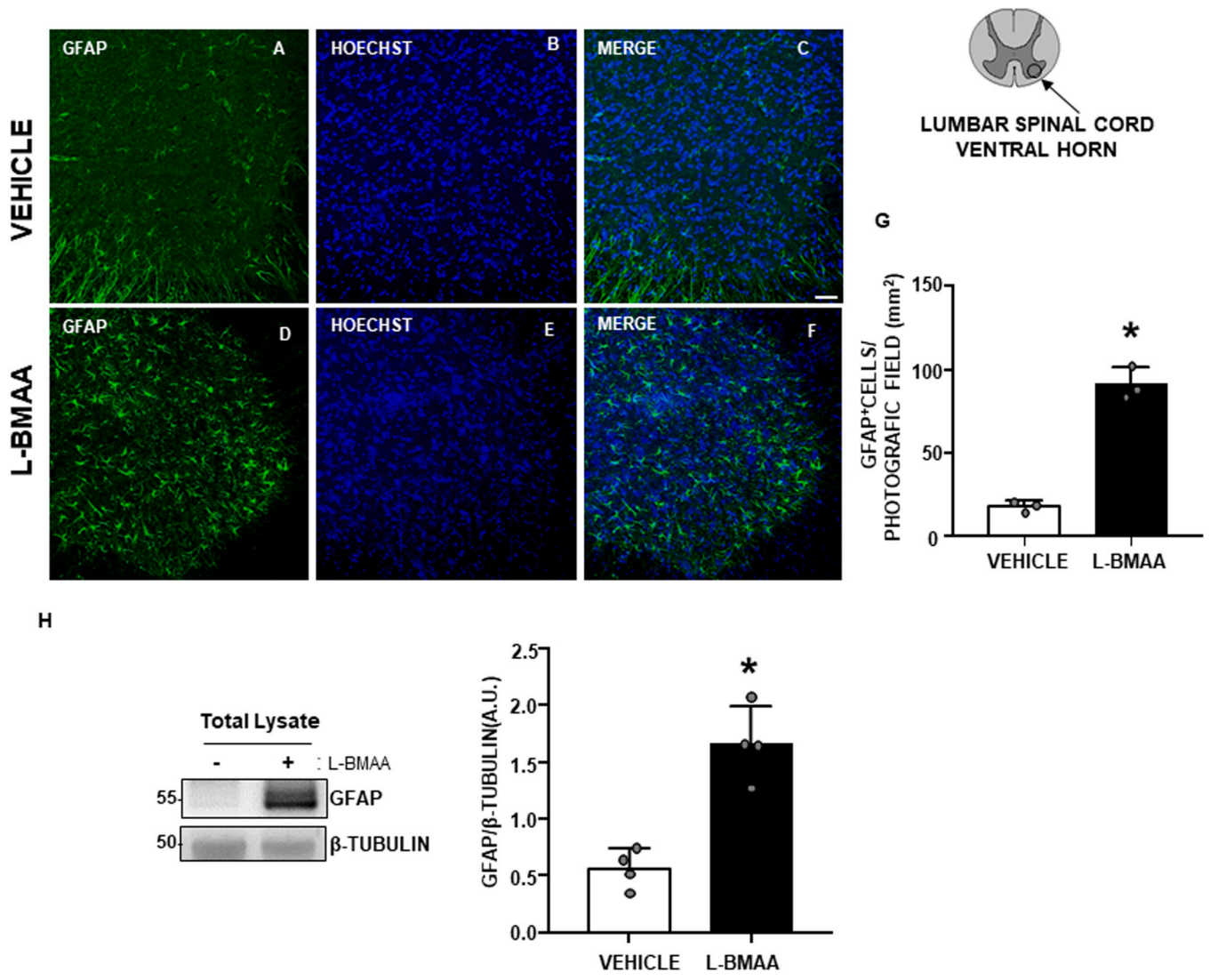

Fig. 5. Evaluation of spinal cord astrogliosis in mice exposed to L-BMAA. A–D) Immunofluorescence analysis of GFAP in spinal cord sections from vehicle or L-BMAA exposed mice. B-E) Nuclei were labeled with Hoechst dye. C-F) Merge images. G) Quantification of total number of activated GFAP cells per photographic field (mm2), arbitrary units (AU). Data are expressed as mean ± SEM (n = 3 for each group). *$p < 0.05$ Error bars ± SEM; for statistical analysis, Student's t test was used, *$p < 0.05$. Original magnification, 10X. Scale bar = 100 μm. H) Representative image of western blot analysis (left panel) and quantification of GFAP protein expression, arbitrary units (AU), (right panel) on total protein extracts from spinal cord. The β-tubulin expression level was used for normalization. Data are expressed as mean ± SEM (n = 4 for each group). *$p < 0.05$

novel object with respect to control animals (Fig. 7D,E), thus indicating no recollection of the encounter with the familiar object during the training session.

Finally, to test repetitive behavior and spatial working memory, mice were challenged with a T-shaped maze. When placed in a novel scenario (represented by the T-maze), mice exhibit interest in exploring different sections of their surroundings, because of their innate exploratory drive. The test consisted in ten subsequent trials, in which mice spent 5 s in the starting box, 60 s of maximum latency to choose to go to the right or left arm of the T-maze, and 30 s confined to the chosen arm (Fig. 7F). As shown in Fig. 7G, L-BMAA-treated mice showed a lower number of alternations between the two arms of the maze compared to the control animals, indicating a higher rate of repetitive behavior, and suggesting spatial memory alteration due to the toxin exposure.

Taken together, these results showed that L-BMAA exposure leads to FTD-like cognitive manifestations in mice.

4. Discussion

In this paper, we characterized for the first time a L-BMAA-induced neurotoxic mouse model of ALS/FTD. In fact, we demonstrated that the chronic administration of the cyanotoxin L-BMAA induces a phenotype that reproduces several ALS/FTD features in mice, such as apoptotic cell death and astrogliosis in spinal cord and motor cortex, increase in TDP-43 expression and cytoplasmic accumulation, and motor and cognitive alterations. Mechanistically, we propose the increase in TDP-43 cytoplasmic expression as one of the main mechanisms responsible for the neurotoxicity of L-BMAA.

There are compelling reasons to investigate ALS risk associated with L-BMAA exposure. In fact, in several world regions drinking water derives primarily from reservoirs mostly eutrophic, with phytoplankton dominated by potentially toxic *Cyanobacteria* [11] and L-BMAA has been detected in natural water samples and in cyanobacterial cell cultures derived from cell isolates from reservoirs [12]. However, the very high doses of L-BMAA required to produce neurotoxicity [34–37] the failure to produce any toxicity in some animal studies have raised questions on

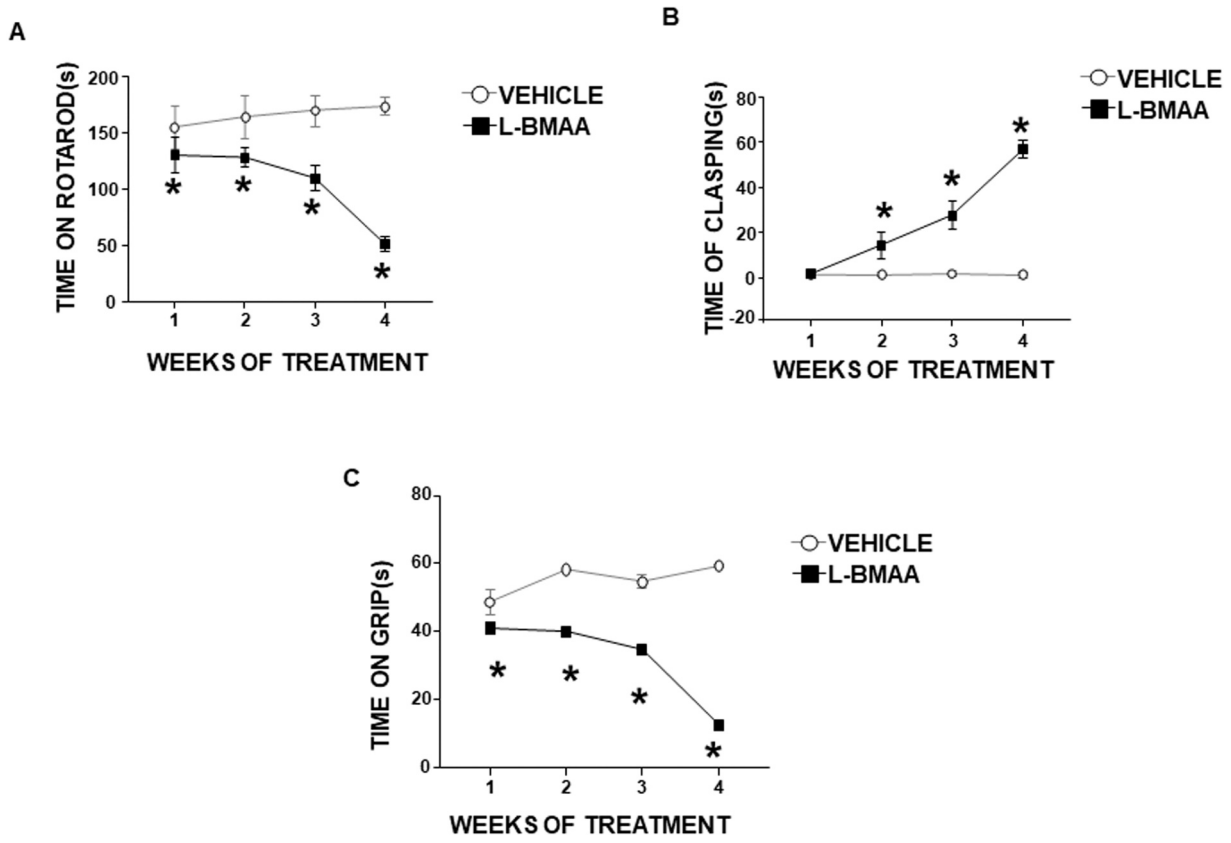

Fig. 6. Effect of L-BMAA exposure on mice motor performance. A) Rotarod test on mice treated with vehicle and L-BMAA. Clasping test in panel B) Grip performance test in panel C) Statistical significance was evaluated using one-way ANOVA with Newman Keuls's correction for multiple comparisons. Data are expressed as mean ± SEM (n = 8 for each group). *$p < 0.05$.

the possible involvement of L-BMAA in ALS/PDC. Despite a renewed interest in the so-called L-BMAA-ALS hypothesis, stimulated by a report showing that several cyanobacterial taxa produce L-BMAA [38], no single mechanism of toxicity has been identified that could justify the development of ALS/PDC and, even at environmentally unattainable exposure regimes, ALS/PDC features and symptoms had not been always adequately reproduced in animal models [39]. Therefore, studying the underlying mechanisms of ALS through an L-BMAA-treated animal model has assumed great relevance in recent years, and multiple doses of L-BMAA have been tested in different species to obtain neurotoxic animal models of ALS. For instance, L-BMAA (25–400 mg/kg) acutely administered to rats by i.v. injection into the femoral or tail vein, or chronically infused into the brain with osmotic mini-pumps could induce neuronal and behavioral changes [39]. More recently, dyskinesia accompanied by the gradual degeneration and loss of MNs, in the anterior horn of the spinal cord and brain motor cortex, has been described in iv L-BMAA-treated rats (300 mg/kg continuous infusion for 3 days). Moreover, L-BMAA exposure in neonatal rats has also caused significant biochemical and behavioural effects [40]. By contrast, another study suggested that chronic oral administration of L-BMAA is not neurotoxic to mice. In fact, a total of 15.5 g/kg of L-BMAA was administered by gavage to mice over 11 weeks without observing any behavioral abnormalities [41]. Similar results on the lack of behavioral and neuropathological effects of dietary L-BMAA in mice were presented by Cruz-Aguado et al.,[19]. The discrepancies among the studies may be due to several factors, including dose, duration of treatment and gender. In fact, over the years, male mice have consistently shown increased sensitivity to L-BMAA toxicity compared to female ones [42], probably because L-BMAA is able to better cross BBB in male than in female mice [43]. This assumption has been further validated by the most recent paper on this topic [44]. This reflects our choice of using only male mice intraperitoneally exposed to L-BMAA for 30 days.

The L-BMAA pharmacokinetics has been studied in several papers showing that brain L-BMAA levels peak within eight hours after injection and decline with a $t_{1/2}$ similar to that of plasma [45]. After two weeks of continuous infusions of L-BMAA (100 mg/ kg per day), brain concentrations reached a steady state and are only moderately higher than those in plasma. This suggests that large doses of L-BMAA may reach potentially toxic levels in the brain (*i.e.* >250 μM) [46]. The latter justifies the choice of the dosage used in the present paper to induce ALS/FTD by chronic administration of L-BMAA. This represents a reliable model of chronic exposure to L-BMAA and a useful model to investigate the molecular features of sporadic ALS cases, since it shows motor deficits and cognitive impairment that were not observed with lower L-BMAA doses [41]. It is noteworthy that several *in vitro* and *in vivo* studies suggest that L-BMAA results in the overexpression of TDP-43 and the formation of protein aggregates, and TDP-43 inclusions have been observed in neurons of two multiple sclerosis patients that presented comorbidity with ALS [25,42]. Loss of nuclear TDP-43 characterizes sporadic and most familial forms of ALS [47] and the accumulation of cytoplasmic TDP-43 is strongly suspected of contributing to MN degeneration in ALS. In fact, under normal conditions, TDP-43 is primarily located in the nucleus, whereas only small amounts exist in the cytosol [48,49]. The accumulation and the aggregation of TDP-43 in the cytoplasm is considered a main driver of ALS and FTD pathogenesis. However, the exact mechanism of such accumulation has not been fully elucidated. Notably, the cytoplasmic accumulation of TDP-43, described also in humans, has been seen also in our L-BMAA model, especially at the late stage after treatment. Furthermore, neuronal loss and an active caspase-3 gene were observed in our model, confirming the role of the cytoplasmic TDP-43 in causing motor neuron death. For all these reasons, the use of our neurotoxic mouse model and

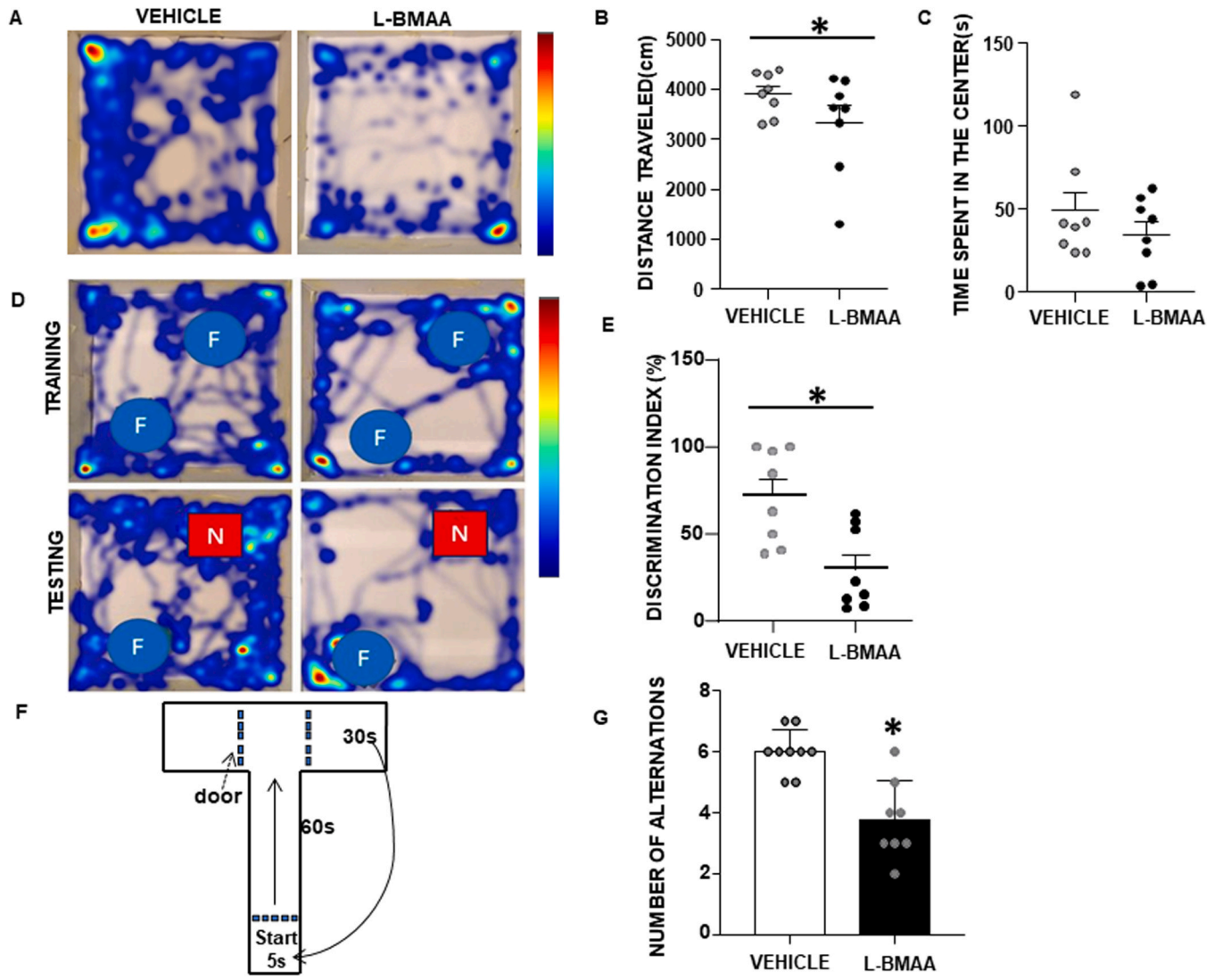

Fig. 7. Effect of L-BMAA exposure on mice cognitive functions. A) Representative image of the mouse trajectory in the open field test. B) Total distance traveled in vehicle and L-BMAA mice. C) Time spent in the center of the arena. D) Representative image of the mouse trajectory in object recognitioning test ("F" stands for familiar, "N" for novel object). E) Discrimination index of novel object expressed as a percentage in vehicle and L-BMAA mice groups. F) Representative image of the T-maze test protocol. G) Total number of alternations in t-maze test. Statistical significance was evaluated using one-way ANOVA with Newman Keuls's correction for multiple comparisons. Data are expressed as mean ± SEM (n = 8 for each group). *$p < 0.05$.

the understanding of the mechanisms of L-BMAA toxicity may be useful for the identification of druggable targets to develop innovative therapeutic strategies for ALS. Remarkably, neurodegenerative diseases such as AD, PD and ALS are all characterized by the appearance of reactive microglial and astroglial cells, which is referred to as neuro-inflammation; and this can contribute to MN death [50]. In our L-BMAA-induced model, GFAP-positive cells infiltration was observed within the parenchyma of the spinal cord and brain motor cortex; and was sustained until the late stage when most of the MNs have undergone apoptosis/necrosis. This is consistent with the opinion that the accumulation of reactive microglia in degenerating areas of ALS tissues is a key cellular event creating a chronic inflammatory environment that results in MN death [51]. Overall, understanding the mechanisms of L-BMAA toxicity may be of relevance to have a versatile, neurotoxic model of ALS and for the identification of druggable targets valuable to develop innovative therapeutic strategies in ALS.

Ethics approval and consent to participate

Not Applicable.

CRediT authors contributions statement

LA, GP, LMTC, SP, GMP and SA conceptualize the paper and designed the experimental procedures; SA, CF, VV, AC, GL, AP and AC carried out *in vitro* experiments; SA, VV, and PB performed *in vivo* experiments: SA, VV, PB, GP and GMP collected data; SA, VV, CF, AC, GL, AP and AC analysed data; LA, GP, LMTC, SP, GMP and SA wrote the paper. All authors read and approved the final manuscript.

Funding

This work was supported by grants from Programma Operativo Nazionale PON PERMEDNET (ArSO1_1226) from the Italian Ministry of Research, MIUR, to LA; PON NEON (ARS01_00769) from the Italian Ministry of Research, MIUR, to GP, by #NEXTGENERATIONEU (NGEU) and funded by the Ministry of University and Research (MUR), National Recovery and Resilience Plan (NRRP), project MNESYS (PE0000006) – A Multiscale integrated approach to the study of the nervous system in health and disease (DN. 1553 11.10.2022) to AC, SP, LA, GMP, GP.

Declaration of Competing Interest

All authors agree that there are no conflicts to declare.

Acknowledgements

We thank Dr. Lucia D'Esposito for her unvaluable support in animal care.

Competing interests

Nothing to declare.

Consent for publication

Not Applicable.

Appendix A. Supporting information

Supplementary data associated with this article can be found in the online version at doi:10.1016/j.biopha.2023.115503.

References

[1] O.M. Peters, M. Ghasemi, R.H. Brown, Emerging mechanisms of molecular pathology in ALS, J. Clin. Invest. 125 (2015) 1767–1779, https://doi.org/10.1172/JCI71601.
[2] S. Sasaki, M. Iwata, Motor neuron disease with predominantly upper extremity involvement: a clinicopathological study, Acta Neuropathol. 98 (1999) 645–650, https://doi.org/10.1007/s004010051131.
[3] G.M. Ringholz, S.H. Appel, M. Bradshaw, N.A. Cooke, D.M. Mosnik, P.E. Schulz, Prevalence and patterns of cognitive impairment in sporadic ALS. Neurology., Neurology. 65(4): (n.d.) 586–590. https://doi.org/5(4):586–90. doi: 10.1212/01.wnl.0000172911.39167.b6. PMID: 16116120.
[4] B.R. Brooks, R.G. Miller, M. Swash, T.L. Munsat, World Federation of Neurology Research Group on Motor Neuron Diseases, El Escorial revisited: revised criteria for the diagnosis of amyotrophic lateral sclerosis, Amyotroph Lateral Scler Other Motor, Neuron Disord 1 (5) (2000) 293–299. PMID: 11464847.
[5] R. Sirabella, V. Valsecchi, S. Anzilotti, O. Cuomo, A. Vinciguerra, P. Cepparulo, P. Brancaccio, N. Guida, N. Blondeau, L.M.T. Canzoniero, C. Franco, S. Amoroso, L. Annunziato, G. Pignataro, Ionic homeostasis maintenance in ALS: Focus on new therapeutic targets, Front. Neurosci. 12 (2018) 1–14, https://doi.org/10.3389/fnins.2018.00510.
[6] S. Saberi, J.E. Stauffer, D.J. Schulte, J. Ravits, Neuropathology of Amyotrophic Lateral Sclerosis and Its Variants, Neurol Clin 33 (4) (2015) 855–876, https://doi.org/10.1016/j.ncl.2015.07.012.
[7] M. Katsuno, F. Tanaka, G. Sobue, Perspectives on molecular targeted therapies and clinical trials for neurodegenerative diseases, J Neurol Neurosurg Psychiatry 83 (3) (2012) 329–335, https://doi.org/10.1136/jnnp-2011-301307. PMID: 22323772.
[8] J. Kim, T.Y. Kim, J.J. Hwang, J.Y. Lee, J.H. Shin, B.J. Gwag, J.Y. Koh, Accumulation of labile zinc in neurons and astrocytes in the spinal cords of G93A SOD-1 transgenic mice, Neurobiol. Dis. 34 (2009) 221–229, https://doi.org/10.1016/j.nbd.2009.01.004.
[9] L. Hiranoa, L.T. Kurland, R.S. Krooth, S.Parkinsonism-dementia complex, an endemic disease on the island of Guam. I. Clinical features., Brain. Clinical features, Brain 84 (1961) 642–661, https://doi.org/10.1093/brain/84.4.642.
[10] A. Moawad, M. Hetta, J.K. Zjawiony, M.R. Jacob, M. Hifnawy, J.P. Marais, D. Ferreira, Phytochemical investigation of Cycas circinalis and Cycas revoluta leaflets: moderately active antibacterial biflavonoids, Planta Med. 76 (8) (2010) 796–802, https://doi.org/10.1055/s-0029-1240743. Epub 2010 Jan 12.
[11] M.A. Mariani, B.M. Padedda, J. Kaštovský, P. Buscarinu, N. Sechi, T. Virdis, A. Lugliè, Effects of trophic status on microcystin production and the dominance of cyanobacteria in the phytoplankton assemblage of Mediterranean reservoirs, Sci. Rep. 5 (2015) 1–16, https://doi.org/10.1038/srep17964.
[12] B. Yan, C. Han, Z. Liu, G. Wu, S. Wang, J. Li, W. Xia, F. Cui, Degradation of cyanobacterial neurotoxin β-N-methylamino-l-alanine (BMAA) using ozone process: influencing factors and mechanism, Environ. Sci. Pollut. Res. 30 (2023) 47873–47881, https://doi.org/10.1007/s11356-023-25754-7.
[13] M.E. Newell, S. Adhikari, R.U. Halden, Systematic and state-of the science review of the role of environmental factors in Amyotrophic Lateral Sclerosis (ALS) or Lou Gehrig's Disease, Sci. Total Environ. 817 (2022), 152504, https://doi.org/10.1016/j.scitotenv.2021.152504.
[14] P.S. Spencer, V.S. Palmer, G.E. Kisby, Western Pacific ALS-PDC: evidence implicating cycad genotoxins, J. Neurol. Sci. 419 (2020), 117185, https://doi.org/10.1016/j.jns.2020.117185.
[15] E.A. Proctor, D.D. Mowrey, N.V. Dokholyan, β-Methylamino-L-alanine substitution of serine in SOD1 suggests a direct role in ALS etiology, PLoS Comput. Biol. 15 (2019) 1–11, https://doi.org/10.1371/journal.pcbi.1007225.
[16] S.A. Banack, P.A. Cox, Creating a simian model of Guam ALS/PDC which reflects chamorro lifetime BMAA exposures, Neurotox. Res. 33 (2018) 24–32, https://doi.org/10.1007/s12640-017-9745-6.
[17] S.A. Banack, J.S. Metcalf, W.G. Bradley, P.A. Cox, Detection of cyanobacterial neurotoxin β-N-methylamino-l-alanine within shellfish in the diet of an ALS patient in Florida, Toxicon 90 (2014) 167–173, https://doi.org/10.1016/j.toxicon.2014.07.018.
[18] S.A. Banack, S.J. Murch, Multiple neurotoxic items in the Chamorro diet link BMAA with ALS/PDC, Amyotroph Lateral Scler 10 (2) (2009) 34–40, https://doi.org/10.3109/17482960903278451.
[19] R. Cruz-Aguado, D. Winkler, C.A. Shaw, Lack of behavioral and neuropathological effects of dietary β-methylamino-l-alanine (BMAA) in mice, Pharmacol. Biochem. Behav. 84 (2006) 294–299, https://doi.org/10.1016/j.pbb.2006.05.012.
[20] S. Anzilotti, P. Brancaccio, G. Simeone, V. Valsecchi, A. Vinciguerra, A. Secondo, T. Petrozziello, N. Guida, R. Sirabella, O. Cuomo, P. Cepparulo, A. Herchuelz, S. Amoroso, G. DI Renzo, L. Annunziato, G. Pignataro, Preconditioning, induced by sub-toxic dose of the neurotoxin L-BMAA, delays ALS progression in mice and prevents Na+/Ca2+ exchanger 3 downregulation, Cell Death Dis. 9 (2018), https://doi.org/10.1038/s41419-017-0227-9.
[21] T. Petrozziello, A. Secondo, V. Tedeschi, A. Esposito, M.J. Sisalli, A. Scorziello, G. Di Renzo, L. Annunziato, ApoSOD1 lacking dismutase activity neuroprotects motor neurons exposed to beta-methylamino-L-alanine through the Ca2+/Akt/ERK1/2 prosurvival pathway, Cell Death Differ. 24 (2017) 511–522, https://doi.org/10.1038/cdd.2016.154.
[22] T. Petrozziello, F. Boscia, V. Tedeschi, A. Pannaccione, V. de Rosa, A. Corvino, B. Severino, L. Annunziato, A. Secondo, Na+/Ca2+ exchanger isoform 1 takes part to the Ca2+-related prosurvival pathway of SOD1 in primary motor neurons exposed to beta-methylamino-l-alanine, Cell Commun. Signal. 20 (2022) 1–12, https://doi.org/10.1186/s12964-021-00813-z.
[23] R.L. French, Z.R. Grese, H. Aligireddy, D.D. Dhavale, A.N. Reeb, N. Kedia, P. T. Kotzbauer, J. Bieschke, Y.M. Ayala, Detection of TAR DNA-binding protein 43 (TDP-43) oligomers as initial intermediate species during aggregate formation, J. Biol. Chem. 294 (2019) 6696–6709, https://doi.org/10.1074/jbc.RA118.005889.
[24] S.C. Ling, M. Polymenidou, D.W. Cleveland, Converging mechanisms in als and FTD: Disrupted RNA and protein homeostasis, Neuron 79 (2013) 416–438, https://doi.org/10.1016/j.neuron.2013.07.033.
[25] K.W. Tian, H. Jiang, B.B. Wang, F. Zhang, S. Han, Intravenous injection of l-BMAA induces a rat model with comprehensive characteristics of amyotrophic lateral sclerosis/Parkinson-dementia complex, Toxicol. Res. (Camb.) 5 (2015) 79–96, https://doi.org/10.1039/c5tx00272a.
[26] G. Bensimon, L. Lacomblez, V. Meininger, A controlled trial of riluzole in amyotrophic lateral sclerosis. ALS/Riluzole Study Group, N Engl J Med. 330 (9) (1994) 585–591, https://doi.org/10.1056/NEJM199403033300901.
[27] H.M. Bryson, P. Benfield, A review of its pharmacodynamic and pharmacokinetic properties and therapeutic potential in amyotrophic lateral sclerosis, Drugs 52 (1996) 549–563, https://doi.org/10.2165/00003495-199652040-00010.
[28] R. Gerlini, E. Amendola, A. Conte, V. Valente, M. Tornincasa, S.C. Credendino, F. Cammarota, C. Gentile, L. Di Guida, S. Paladino, G. De Vita, G.M. Pierantoni, A. Fusco, Double knock-out of Hmga1 and Hipk2 genes causes perinatal death associated to respiratory distress and thyroid abnormalities in mice, Cell Death Dis. 10 (2019), https://doi.org/10.1038/s41419-019-1975-5.
[29] S. Anzilotti, V. Valsecchi, P. Brancaccio, N. Guida, G. Laudati, V. Tedeschi, T. Petrozziello, F. Frecentese, E. Magli, B. Hassler, O. Cuomo, L. Formisano, A. Secondo, L. Annunziato, G. Pignataro, Prolonged NCX activation prevents SOD1 accumulation, reduces neuroinflammation, ameliorates motor behavior and prolongs survival in a ALS mouse model, Neurobiol. Dis. 159 (2021), 105480, https://doi.org/10.1016/j.nbd.2021.105480.
[30] V. Valsecchi, S. Anzilotti, A. Serani, G. Laudati, P. Brancaccio, N. Guida, O. Cuomo, G. Pignataro, L. Annunziato, miR-206 reduces the severity of motor neuron degeneration in the facial nuclei of the brainstem in a mouse model of SMA, Mol. Ther. 28 (2020) 1154–1166, https://doi.org/10.1016/j.ymthe.2020.01.013.
[31] P. Cerullo, P. Brancaccio, S. Anzilotti, A. Vinciguerra, O. Cuomo, F. Fiorino, B. Severino, P. Di Vaio, G. Di Renzo, L. Annunziato, G. Pignataro, Acute and long-term NCX activation reduces brain injury and restores behavioral functions in mice subjected to neonatal brain ischemia, Neuropharmacology 135 (2018) 180–191, https://doi.org/10.1016/j.neuropharm.2018.03.017.
[32] N. Guida, G. Laudati, S. Anzilotti, R. Sirabella, O. Cuomo, P. Brancaccio, M. Santopaolo, M. Galgani, P. Montuori, G. Di Renzo, L.M.T. Canzoniero, L. Formisano, Methylmercury upregulates RE-1 silencing transcription factor (REST) in SH-SY5Y cells and mouse cerebellum, Neurotoxicology 52 (2016) 89–97, https://doi.org/10.1016/j.neuro.2015.11.007.
[33] S. Natale, S. Anzilotti, T. Petrozziello, R. Ciccone, A. Serani, L. Calabrese, B. Severino, F. Frecentese, A. Secondo, A. Pannaccione, F. Fiorino, O. Cuomo, A. Vinciguerra, L. D'Esposito, A.G. Sadile, S. Cabib, G. Di Renzo, L. Annunziato, P. Molinaro, Genetic Up-Regulation or Pharmacological Activation of the Na+/Ca2+ Exchanger 1 (NCX1) Enhances Hippocampal-Dependent Contextual and Spatial Learning and Memory, Mol. Neurobiol. 57 (2020) 2358–2376, https://doi.org/10.1007/s12035-020-01888-4.
[34] P.B. Nunn, Three phases of research on beta-N-methylamino-L-alanine (BMAA)–a neurotoxic amino acid, Amyotroph Lateral Scler 10 (2) (2009) 26–33, https://doi.org/10.3109/17482960903272975. PMID: 19929728.
[35] J.H. Weiss, D.W. Choi, Beta-N-methylamino-L-alanine neurotoxicity: requirement for bicarbonate as a cofactor, Science 241 (4868) (1988) 973–975, https://doi.org/10.1126/science.3136549. PMID: 3136549.

[36] S.M. Ross, P.S. Spencer, Specific antagonism of behavioral action of "uncommon" amino acids linked to motor-system diseases, Synapse 1 (3) (1987) 248–253, https://doi.org/10.1002/syn.890010305. PMID: 3145580.
[37] M. Lee, P.L. McGeer, Weak BMAA toxicity compares with that of the dietary supplement β-alanine, Neurobiol Aging 33 (7) (2012) 1440–1447, https://doi.org/10.1016/j.neurobiolaging.2010.11.024. Epub 2011 Jan 13. PMID: 21236519.
[38] P.A. Cox, S.A. Banack, S.J. Murch, U. Rasmussen, G. Tien, R.R. Bidigare, J. S. Metcalf, L.F. Morrison, G.A. Codd, B. Bergman, Diverse taxa of cyanobacteria produce β-N-methylamino-L-alanine, a neurotoxic amino acid, Proc. Natl. Acad. Sci. USA 102 (2005) 5074–5078, https://doi.org/10.1073/pnas.0501526102.
[39] V.T. Karamyan, R.C. Speth, Animal models of BMAA neurotoxicity: a critical review, Life Sci. 82 (2008) 233–246, https://doi.org/10.1016/j.lfs.2007.11.020.
[40] M.K.R. Engskog, O. Karlsson, J. Haglöf, A. Elmsjö, E. Brittebo, T. Arvidsson, C. Pettersson, The cyanobacterial amino acid β-N-methylamino-l-alanine perturbs the intermediary metabolism in neonatal rats, Toxicology 312 (2013) 6–11, https://doi.org/10.1016/j.tox.2013.07.010.
[41] T.L. Perry, C. Bergeron, A.J. Biro, S. Hansen, β-N-Methylamino-l-alanine. Chronic oral administration is not neurotoxic to mice, J. Neurol. Sci. 94 (1989) 173–180, https://doi.org/10.1016/0022-510X(89)90227-X.
[42] L.L. Scott, T.G. Downing, A single neonatal exposure to BMAA in a rat model produces neuropathology consistent with neurodegenerative diseases, Toxins 10 (2018) 18–23, https://doi.org/10.3390/toxins10010022.
[43] M.A. Al-Sammak, D.G. Rogers, K.D. Hoagland, Acute β - N -Methylamino-L-alanine toxicity in a mouse model, J. Toxicol. 2015 (2015), https://doi.org/10.1155/2015/739746.
[44] F.J. Arnold, M. Burns, Y. Chiu, J. Carvalho, A.D. Nguyen, P.C. Ralph, A.R. La Spada, C.L. Bennett, Chronic BMAA exposure combined with TDP-43 mutation elicits motor neuron dysfunction phenotypes in mice, Neurobiol. Aging 126 (2023) 44–57, https://doi.org/10.1016/j.neurobiolaging.2023.02.010.
[45] M.W. Duncan, N.E. Villacreses, P.G. Pearson, L. Wyatt, S.I. Rapoport, I.J. Kopin, S. P. Markey, Q.R. Smith, 2-amino-3-(methylamino)-propanoic acid (BMAA) pharmacokinetics and blood-brain barrier permeability in the rat, J Pharmacol Exp Ther. 258 (1) (1991) 27–35. PMID: 2072299.
[46] M.W. Duncan, S.P. Markey, B.G. Weick, P.G. Pearson, H. Ziffer, Y. Hu, I.J. Kopin, 2-Amino-3-(methylamino)propanoic acid (BMAA) bioavailability in the primate, Neurobiol Aging 13 (2) (1992) 333–337, https://doi.org/10.1016/0197-4580(92)90047-2. PMID: 1522948.
[47] J.R. Highley, J. Kirby, J.A. Jansweijer, P.S. Webb, C.A. Hewamadduma, P.R. Heath, A. Higginbottom, R. Raman, L. Ferraiuolo, J. Cooper-Knock, C.J. Mcdermott, S. B. Wharton, P.J. Shaw, P.G. Ince, Loss of nuclear TDP-43 in amyotrophic lateral sclerosis (ALS) causes altered expression of splicing machinery and widespread dysregulation of RNA splicing in motor neurones, Neuropathol. Appl. Neurobiol. 40 (2014) 670–685, https://doi.org/10.1111/nan.12148.
[48] H.Z. Yin, S. Yu, C.I. Hsu, J. Liu, A. Acab, R. Wu, A. Tao, B.J. Chiang, J.H. Weiss, Intrathecal infusion of BMAA induces selective motor neuron damage and astrogliosis in the ventral horn of the spinal cord, Exp. Neurol. 261 (2014) 1–9, https://doi.org/10.1016/j.expneurol.2014.06.003.
[49] E. De Munck, E. Muñoz-Sáez, B.G. Miguel, M.T. Solas, I. Ojeda, A. Martínez, C. Gil, R.M. Arahuetes, β-N-methylamino-l-alanine causes neurological and pathological phenotypes mimicking Amyotrophic Lateral Sclerosis (ALS): the first step towards an experimental model for sporadic ALS, Environ. Toxicol. Pharmacol. 36 (2013) 243–255, https://doi.org/10.1016/j.etap.2013.04.007.
[50] T. Philips, W. Robberecht, Neuroinflammation in amyotrophic lateral sclerosis: Role of glial activation in motor neuron disease, Lancet Neurol. 10 (2011) 253–263, https://doi.org/10.1016/S1474-4422(11)70015-1.
[51] F. González-Scarano, G. Baltuch, Microglia as mediators of inflammatory and degenerative diseases, Annu. Rev. Neurosci. 22 (1999) 219–240, https://doi.org/10.1146/annurev.neuro.22.1.219.